EUROPEAN ORGANIZATION FOR NUCLEAR RESEARCH

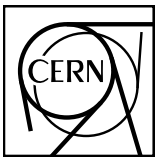

CERN-EP-2018-012v2
October 9, 2018

K^- over K^+ multiplicity ratio for kaons produced in DIS with a large fraction of the virtual-photon energy

The COMPASS Collaboration

Abstract

The K^- over K^+ multiplicity ratio is measured in deep-inelastic scattering, for the first time for kaons carrying a large fraction z of the virtual-photon energy. The data were obtained by the COMPASS collaboration using a 160 GeV muon beam and an isoscalar ^{6}LiD target. The regime of deep-inelastic scattering is ensured by requiring $Q^2 > 1$ (GeV/c)^2 for the photon virtuality and $W > 5$ GeV/c^2 for the invariant mass of the produced hadronic system. Kaons are identified in the momentum range from 12 GeV/c to 40 GeV/c, thereby restricting the range in Bjorken-x to $0.01 < x < 0.40$. The z-dependence of the multiplicity ratio is studied for $z > 0.75$. For very large values of z, *i.e.* $z > 0.8$, we observe the kaon multiplicity ratio to fall below the lower limits expected from calculations based on leading and next-to-leading order perturbative quantum chromodynamics. Also, the kaon multiplicity ratio shows a strong dependence on the missing mass of the single-kaon production process. This suggests that within the perturbative quantum chromodynamics formalism an additional correction may be required, which takes into account the phase space available for hadronisation.

(to be submitted to Phys. Lett. B)

The COMPASS Collaboration

R. Akhunzyanov[7], M.G. Alexeev[25], G.D. Alexeev[7], A. Amoroso[25,26], V. Andrieux[28,20], N.V. Anfimov[7], V. Anosov[7], A. Antoshkin[7], K. Augsten[7,18], W. Augustyniak[29], A. Austregesilo[15], C.D.R. Azevedo[1], B. Badełek[30], F. Balestra[25,26], M. Ball[3], J. Barth[4], R. Beck[3], Y. Bedfer[20], J. Bernhard[12,9], K. Bicker[15,9], E. R. Bielert[9], R. Birsa[24], M. Bodlak[17], P. Bordalo[11,a], F. Bradamante[23,24], A. Bressan[23,24], M. Büchele[8], V.E. Burtsev[27], L. Capozza[20], W.-C. Chang[21], C. Chatterjee[6], M. Chiosso[25,26], A.G. Chumakov[27], S.-U. Chung[15,b], A. Cicuttin[24,c], M.L. Crespo[24,c], Q. Curiel[20], S. Dalla Torre[24], S.S. Dasgupta[6], S. Dasgupta[23,24], O.Yu. Denisov[26,#], L. Dhara[6], S.V. Donskov[19], N. Doshita[32], Ch. Dreisbach[15], W. Dünnweber[d], R.R. Dusaev[27], M. Dziewiecki[31], A. Efremov[7,r], P.D. Eversheim[3], M. Faessler[d], A. Ferrero[20], M. Finger[17], M. Finger jr.[17], H. Fischer[8], C. Franco[11], N. du Fresne von Hohenesche[12,9], J.M. Friedrich[15,#], V. Frolov[7,9], F. Gautheron[2], O.P. Gavrichtchouk[7], S. Gerassimov[14,15], J. Giarra[12], I. Gnesi[25,26], M. Gorzellik[8,m], A. Grasso[25,26], A. Gridin[7], M. Grosse Perdekamp[28], B. Grube[15], A. Guskov[7], D. Hahne[4], G. Hamar[24], D. von Harrach[12], R. Heitz[28], F. Herrmann[8], N. Horikawa[16,e], N. d'Hose[20], C.-Y. Hsieh[21,f], S. Huber[15], S. Ishimoto[32,g], A. Ivanov[25,26], T. Iwata[32], V. Jary[18], R. Joosten[3], P. Jörg[8], E. Kabuß[12], A. Kerbizi[23,24], B. Ketzer[3],G.V. Khaustov[19], Yu.A. Khokhlov[19,h], Yu. Kisselev[7], F. Klein[4], J.H. Koivuniemi[2,28], V.N. Kolosov[19], K. Kondo[32], I. Konorov[14,15], V.F. Konstantinov[19], A.M. Kotzinian[26,j], O.M. Kouznetsov[7], Z. Kral[18], M. Krämer[15], F. Krinner[15], Z.V. Kroumchtein[7,*], Y. Kulinich[28], F. Kunne[20], K. Kurek[29], R.P. Kurjata[31], I.I. Kuznetsov[27], A. Kveton[18], A.A. Lednev[19,*], E.A. Levchenko[27], S. Levorato[24], Y.-S. Lian[21,k], J. Lichtenstadt[22], R. Longo[25,26], V.E. Lyubovitskij[27], A. Maggiora[26], A. Magnon[28], N. Makins[28], N. Makke[24,c], G.K. Mallot[9], S.A. Mamon[27], C. Marchand[20], B. Marianski[29], A. Martin[23,24], J. Marzec[31], J. Matoušek[23,24,17], H. Matsuda[32], T. Matsuda[13], G.V. Meshcheryakov[7], M. Meyer[28,20], W. Meyer[2], Yu.V. Mikhailov[19], M. Mikhasenko[3], E. Mitrofanov[7], N. Mitrofanov[7], Y. Miyachi[32], A. Moretti[23], A. Nagaytsev[7], F. Nerling[12], D. Neyret[20], J. Nový[18,9], W.-D. Nowak[12], G. Nukazuka[32], A.S. Nunes[11], A.G. Olshevsky[7], I. Orlov[7], M. Ostrick[12], D. Panzieri[26,l], B. Parsamyan[25,26], S. Paul[15], J.-C. Peng[28], F. Pereira[1], G. Pesaro[23,24], M. Pešek[17], M. Pešková[17], D.V. Peshekhonov[7], N. Pierre[12,20], S. Platchkov[20], J. Pochodzalla[12], V.A. Polyakov[19], J. Pretz[4,i], M. Quaresma[11], C. Quintans[11], S. Ramos[11,a], C. Regali[8], G. Reicherz[2], C. Riedl[28], D.I. Ryabchikov[19,15], A. Rybnikov[7], A. Rychter[31], R. Salac[18], V.D. Samoylenko[19], A. Sandacz[29], S. Sarkar[6], I.A. Savin[7,r], T. Sawada[21], G. Sbrizzai[23,24], P. Schiavon[23,24], H. Schmieden[4], E. Seder[20], A. Selyunin[7], L. Silva[11], L. Sinha[6], S. Sirtl[8], M. Slunecka[7], F. Sozzi[24] J. Smolik[7], A. Srnka[5], D. Steffen[9,15], M. Stolarski[11,#], O. Subrt[9,18], M. Sulc[10], H. Suzuki[32,e], A. Szabelski[23,24,29] T. Szameitat[8,m], P. Sznajder[29], M. Tasevsky[7], S. Tessaro[24], F. Tessarotto[24], A. Thiel[3], J. Tomsa[17], F. Tosello[26], V. Tskhay[14], S. Uhl[15], B.I. Vasilishin[27], A. Vauth[9], B.M. Veit[12], J. Veloso[1], A. Vidon[20], M. Virius[18], S. Wallner[15], M. Wilfert[12], R. Windmolders[4], K. Zaremba[31], P. Zavada[7], M. Zavertyaev[14], E. Zemlyanichkina[7,r], M. Ziembicki[31]

[1] University of Aveiro, Dept. of Physics, 3810-193 Aveiro, Portugal
[2] Universität Bochum, Institut für Experimentalphysik, 44780 Bochum, Germany[n,o]
[3] Universität Bonn, Helmholtz-Institut für Strahlen- und Kernphysik, 53115 Bonn, Germany[n]
[4] Universität Bonn, Physikalisches Institut, 53115 Bonn, Germany[n]
[5] Institute of Scientific Instruments, AS CR, 61264 Brno, Czech Republic[p]
[6] Matrivani Institute of Experimental Research & Education, Calcutta-700 030, India[q]
[7] Joint Institute for Nuclear Research, 141980 Dubna, Moscow region, Russia[r]
[8] Universität Freiburg, Physikalisches Institut, 79104 Freiburg, Germany[n,o]
[9] CERN, 1211 Geneva 23, Switzerland
[10] Technical University in Liberec, 46117 Liberec, Czech Republic[p]
[11] LIP, 1000-149 Lisbon, Portugal[s]
[12] Universität Mainz, Institut für Kernphysik, 55099 Mainz, Germany[n]

[13] University of Miyazaki, Miyazaki 889-2192, Japan[t]
[14] Lebedev Physical Institute, 119991 Moscow, Russia
[15] Technische Universität München, Physik Dept., 85748 Garching, Germany[n,d]
[16] Nagoya University, 464 Nagoya, Japan[t]
[17] Charles University in Prague, Faculty of Mathematics and Physics, 18000 Prague, Czech Republic[p]
[18] Czech Technical University in Prague, 16636 Prague, Czech Republic[p]
[19] State Scientific Center Institute for High Energy Physics of National Research Center 'Kurchatov Institute', 142281 Protvino, Russia
[20] IRFU, CEA, Université Paris-Saclay, 91191 Gif-sur-Yvette, France[o]
[21] Academia Sinica, Institute of Physics, Taipei 11529, Taiwan[u]
[22] Tel Aviv University, School of Physics and Astronomy, 69978 Tel Aviv, Israel[v]
[23] University of Trieste, Dept. of Physics, 34127 Trieste, Italy
[24] Trieste Section of INFN, 34127 Trieste, Italy
[25] University of Turin, Dept. of Physics, 10125 Turin, Italy
[26] Torino Section of INFN, 10125 Turin, Italy
[27] Tomsk Polytechnic University,634050 Tomsk, Russia[w]
[28] University of Illinois at Urbana-Champaign, Dept. of Physics, Urbana, IL 61801-3080, USA[x]
[29] National Centre for Nuclear Research, 00-681 Warsaw, Poland[y]
[30] University of Warsaw, Faculty of Physics, 02-093 Warsaw, Poland[y]
[31] Warsaw University of Technology, Institute of Radioelectronics, 00-665 Warsaw, Poland[y]
[32] Yamagata University, Yamagata 992-8510, Japan[t]

[#] Corresponding authors
[*] Deceased
[a] Also at Instituto Superior Técnico, Universidade de Lisboa, Lisbon, Portugal
[b] Also at Dept. of Physics, Pusan National University, Busan 609-735, Republic of Korea and at Physics Dept., Brookhaven National Laboratory, Upton, NY 11973, USA
[c] Also at Abdus Salam ICTP, 34151 Trieste, Italy
[d] Supported by the DFG cluster of excellence 'Origin and Structure of the Universe' (www.universe-cluster.de) (Germany)
[e] Also at Chubu University, Kasugai, Aichi 487-8501, Japan[t]
[f] Also at Dept. of Physics, National Central University, 300 Jhongda Road, Jhongli 32001, Taiwan
[g] Also at KEK, 1-1 Oho, Tsukuba, Ibaraki 305-0801, Japan
[h] Also at Moscow Institute of Physics and Technology, Moscow Region, 141700, Russia
[i] Present address: RWTH Aachen University, III. Physikalisches Institut, 52056 Aachen, Germany
[j] Also at Yerevan Physics Institute, Alikhanian Br. Street, Yerevan, Armenia, 0036
[k] Also at Dept. of Physics, National Kaohsiung Normal University, Kaohsiung County 824, Taiwan
[l] Also at University of Eastern Piedmont, 15100 Alessandria, Italy
[m] Supported by the DFG Research Training Group Programmes 1102 and 2044 (Germany)
[n] Supported by BMBF - Bundesministerium für Bildung und Forschung (Germany)
[o] Supported by FP7, HadronPhysics3, Grant 283286 (European Union)
[p] Supported by MEYS, Grant LG13031 (Czech Republic)
[q] Supported by B.Sen fund (India)
[r] Supported by CERN-RFBR Grant 12-02-91500
[s] Supported by FCT - Fundação para a Ciência e Tecnologia, COMPETE and QREN, Grants CERN/FP 116376/2010, 123600/2011 and CERN/FIS-NUC/0017/2015 (Portugal)
[t] Supported by MEXT and JSPS, Grants 18002006, 20540299, 18540281 and 26247032, the Daiko and Yamada Foundations (Japan)
[u] Supported by the Ministry of Science and Technology (Taiwan)
[v] Supported by the Israel Academy of Sciences and Humanities (Israel)

[w] Supported by the Russian Federation program “Nauka” (Contract No. 0.1764.GZB.2017) (Russia)
[x] Supported by the National Science Foundation, Grant no. PHY-1506416 (USA)
[y] Supported by NCN, Grant 2015/18/M/ST2/00550 (Poland)

1 Introduction

Quark fragmentation into hadrons is a process of fundamental nature. In perturbative quantum chromodynamics (pQCD), this process is effectively described by non-perturbative objects called fragmentation functions (FFs). While these functions presently cannot be predicted by theory, their scale evolution is described by the DGLAP equations [1]. In leading order (LO) pQCD, the FF $D_{\mathrm{q}}^{\mathrm{h}}$ represents a probability density, which describes the scaled momentum distribution of a hadron type h that is produced in the fragmentation of a quark with flavour q.

The cleanest way to access FFs is to study hadron production in single-inclusive annihilation, $e^+ + e^- \to \mathrm{h} + X$, where the remaining final state X is not analysed. These studies have two disadvantages: *i*) that only information about $D_{\mathrm{q}}^{\mathrm{h}} + D_{\bar{\mathrm{q}}}^{\mathrm{h}}$ is accessible, and *ii*) without invoking model-dependent algorithms for quark-flavour tagging only limited flavour separation is possible. In contrast, the analysis of semi-inclusive measurements of deep-inelastic lepton-nucleon scattering (SIDIS) is advantageous in that q and $\bar{\mathrm{q}}$ can be accessed separately and full flavour separation is possible in principle. Here, the disadvantage is that in the pQCD description of a SIDIS measurement FFs appear convoluted with parton distribution functions (PDFs).

Recently, COMPASS reported results on charged-hadron, pion and kaon multiplicities obtained over a wide kinematic range [2, 3]. These results provide important input for phenomenological analyses of FFs. The pion multiplicities were found to be well described both in leading-order (LO) and next-to-leading order (NLO) pQCD, while this was not the case for kaon multiplicities. The region of large z appears to be particularly problematic for kaons, as it was also observed in subsequent analyses [4] of the COMPASS multiplicities. Here, z denotes the fraction of the virtual-photon energy carried by the produced hadron in the target rest frame.

In this Letter, we present results on the K^- over K^+ multiplicity ratio in the large-z region, *i.e.* for $z > 0.75$. Instead of studying multiplicities for K^- and K^+ separately, their ratio R_{K} is analysed as in this case most experimental systematic effects cancel. Similarly, the impact of theoretical uncertainties, *e.g.* scale uncertainties, is largely reduced in the ratio. Also, while pQCD cannot predict values of multiplicities, limits for certain multiplicity ratios can be predicted. The Letter is organised as follows: in Section 2 various predictions for R_{K} are discussed. The experimental set-up and the data selection are described in Section 3. The analysis method is presented in Section 4, followed by the discussion of the systematic uncertainties in Section 5. The results are presented and discussed in Section 6.

2 Theoretical framework and model expectations

Hadrons of type h produced in a SIDIS measurement are commonly characterised by their relative abundance. The hadron multiplicity M^{h} is defined as the ratio of the SIDIS cross section for hadron type h to the cross section for an inclusive measurement of the deep-inelastic scattering process:

$$\frac{\mathrm{d}M^{\mathrm{h}}(x,Q^2,z)}{\mathrm{d}z} = \frac{\mathrm{d}^3\sigma^{\mathrm{h}}(x,Q^2,z)/\mathrm{d}x\mathrm{d}Q^2\mathrm{d}z}{\mathrm{d}^2\sigma^{\mathrm{DIS}}(x,Q^2)/\mathrm{d}x\mathrm{d}Q^2}. \tag{1}$$

Here, Q^2 is the virtuality of the photon mediating the lepton-nucleon scattering process and x denotes the Bjorken scaling variable. Within the standard factorisation approach of pQCD [5, 6], σ^{DIS} can be written as a sum over parton types, in which for a given parton type a the respective PDF is convoluted with the lepton-parton hard-scattering cross section. For σ^{h} in the current fragmentation region, the sum contains an additional convolution with the fragmentation function of the produced parton. The rather complicated NLO expressions for these cross sections can be found *e.g.* in Ref. [6]. Below, we will use only pQCD LO expressions for the cross section, while later for the presentation of results also multiplicity calculations obtained using NLO expressions will be shown. It is important to note that in the SIDIS factorisation approach the only ingredients that depend on the nucleon type are the nucleon PDFs,

while the fragmentation functions depend neither on the nucleon type nor on x. In the LO approximation for the multiplicity, the sum over parton species $a = \mathrm{q}, \bar{\mathrm{q}}$ does not contain convolutions but only simple products of PDFs $f_a(x,Q^2)$, weighted by the square of the electric charge e_a of the quark expressed in units of elementary charge, and FFs $D_a^{\mathrm{h}}(z,Q^2)$:

$$\frac{\mathrm{d}M^{\mathrm{h}}(x,Q^2,z)}{\mathrm{d}z} = \frac{\sum_a e_a^2 f_a(x,Q^2) D_a^{\mathrm{h}}(z,Q^2)}{\sum_a e_a^2 f_a(x,Q^2)}. \tag{2}$$

For a deuteron target, the charged-kaon multiplicity ratio in LO pQCD reads as follows:

$$R_{\mathrm{K}}(x,Q^2,z) = \frac{\mathrm{d}M^{\mathrm{K}^-}(x,Q^2,z)/\mathrm{d}z}{\mathrm{d}M^{\mathrm{K}^+}(x,Q^2,z)/\mathrm{d}z} = \frac{4(\bar{\mathrm{u}}+\bar{\mathrm{d}})D_{\mathrm{fav}} + (5\mathrm{u}+5\mathrm{d}+\bar{\mathrm{u}}+\bar{\mathrm{d}}+2\bar{\mathrm{s}})D_{\mathrm{unf}} + 2\mathrm{s}D_{\mathrm{str}}}{4(\mathrm{u}+\mathrm{d})D_{\mathrm{fav}} + (5\bar{\mathrm{u}}+5\bar{\mathrm{d}}+\mathrm{u}+\mathrm{d}+2\mathrm{s})D_{\mathrm{unf}} + 2\bar{\mathrm{s}}D_{\mathrm{str}}}. \tag{3}$$

Here, u, $\bar{\mathrm{u}}$, d, $\bar{\mathrm{d}}$, s, $\bar{\mathrm{s}}$ denote the PDFs in the proton for different quark flavours. Their dependences on x and Q^2 are omitted for brevity. The symbols D_{fav}, D_{unf} and D_{str} denote favoured, unfavoured, and strange-quark fragmentation functions respectively, which are given by $D_{\mathrm{fav}} = D_{\mathrm{u}}^{\mathrm{K}^+} = D_{\bar{\mathrm{u}}}^{\mathrm{K}^-}$, $D_{\mathrm{unf}} = D_{\bar{\mathrm{u}}}^{\mathrm{K}^+} = D_{\mathrm{d}}^{\mathrm{K}^+} = D_{\bar{\mathrm{d}}}^{\mathrm{K}^+} = D_{\mathrm{s}}^{\mathrm{K}^+}$ and their charge conjugate, and $D_{\mathrm{str}} = D_{\bar{\mathrm{s}}}^{\mathrm{K}^+} = D_{\mathrm{s}}^{\mathrm{K}^-}$. Their dependences on z and Q^2 are omitted. Accordingly, also the dependence of R_{K} on x, Q^2 and z are omitted. Presently, existing data do not allow one to distinguish between different functions D_{unf} for different quark flavours. However, it is expected that D_{unf} is small in the large-z region, and this expectation is indeed confirmed in pQCD fits already at moderate values of z, *i.e.* $z \approx 0.5$, see e.g. Refs. [7, 8]. When neglecting D_{unf}, Eq. (3) simplifies to

$$R_{\mathrm{K}} = \frac{4(\bar{\mathrm{u}}+\bar{\mathrm{d}})D_{\mathrm{fav}} + 2\mathrm{s}D_{\mathrm{str}}}{4(\mathrm{u}+\mathrm{d})D_{\mathrm{fav}} + 2\bar{\mathrm{s}}D_{\mathrm{str}}}. \tag{4}$$

It is expected that $D_{\mathrm{str}} > D_{\mathrm{fav}} > 0$, and therefore the positive terms $\mathrm{s}D_{\mathrm{str}}$ and $\bar{\mathrm{s}}D_{\mathrm{str}}$ may be of some importance. Still, in order to calculate a lower limit for R_{K}, these terms can be neglected under the assumption that $\mathrm{s} = \bar{\mathrm{s}}$, which leads to

$$R_{\mathrm{K}} > \frac{\bar{\mathrm{u}}+\bar{\mathrm{d}}}{\mathrm{u}+\mathrm{d}}. \tag{5}$$

The analysis described below is performed using two bins in x, *i.e.* $x < 0.05$ with $\langle x \rangle = 0.03$, $\langle Q^2 \rangle = 1.6$ $(\mathrm{GeV}/c)^2$ and $x > 0.05$ with $\langle x \rangle = 0.094$, $\langle Q^2 \rangle = 4.8$ $(\mathrm{GeV}/c)^2$. Whenever sufficient, only the first x-bin is used in the discussion.

The evaluation of Eq. (5) for $x = 0.03$ and $Q^2 = 1.6$ $(\mathrm{GeV}/c)^2$ yields a lower limit of 0.469 ± 0.015 when using the MSTW08 LO PDFs [9]. In NLO the limit given by Eq. (5) receives corrections on the level of $\sim \alpha_S/2\pi$. Using the MMHT14 NLO PDF set [10], the ratio $(\bar{\mathrm{u}}+\bar{\mathrm{d}})/(\mathrm{u}+\mathrm{d})$ is 0.440 ± 0.023, but according to our calculation the lower limit is about 15% lower than this limit [1].

We note that because of the large uncertainties of $\mathrm{s}, \bar{\mathrm{s}}$ and D_{str}, reasonable uncertainties are presently calculable only for the lower limits of R_{K}, and not for R_{K} itself. These uncertainties amount to about 3% for LO and about 6% for NLO predictions. In both cases the uncertainty of the $(\bar{\mathrm{u}}+\bar{\mathrm{d}})/(\mathrm{u}+\mathrm{d})$ ratio dominates, while in NLO also uncertainties of the gluon PDF play some role. The choice of FFs has negligible impact on LO or NLO calculations of the lower R_{K} limit. The actual predictions for R_{K}

[1] From the formalism given in [5], it follows that in the NLO cross-section formula for hadron production, for each quark flavour there are six additional terms besides the $\mathrm{q}D_{\mathrm{q}}^{\mathrm{h}}$ term. These terms include convolution integrals of of PDF, FFs and the so-called coefficient functions. We found that four convolution integrals can effectively be neglected at high z, and only two that are related to convolutions of C_{qq}^1 and C_{qg}^1 have an important impact on the final results. The term related to C_{qq}^1 alone would lead to an increase of R_{K} above the limit given by Eq. (5). In contrast, the term related to C_{qg}^1, although appearing in a symmetric form in numerator and denominator, is negative, so that the lower limit of R_{K} falls below that given by Eq. (5). We note that D_{fav} or its convolution appears always in all relevant terms. Its choice hence appears to be rather irrelevant for the final result, as it largely cancels in the predicted lower limit for R_{K} at NLO.

based on DSS [7] at LO accuracy and DEHSS17 [8] at NLO accuracy are larger than the lower limits for R_{K}, which is expected as in the above calculation of lower limits the strange-quark contribution to kaon fragmentation was neglected. It was verified that when using more recent PDF sets (*e.g.* NNPDF30 at LO and NLO accuracy [11]), the R_{K} values increase by about 10% for all cases that were discussed above. Hence our choice of the MSTW08 LO and MMHT14 NLO PDFs sets leads to a rather conservative estimation of the lower limit on R_{K}.

In the LEPTO event generator [2] [12]. another factorisation ansatz is used

$$\frac{\mathrm{d}M^{\mathrm{h}}(x,Q^2,z)}{\mathrm{d}z} = \frac{\sum_a e_a^2 f_a(x,Q^2) H^{\mathrm{h}}_{a/N}(x,z,Q^2)}{\sum_a e_a^2 f_a(x,Q^2)}. \tag{6}$$

Here, $H^{\mathrm{h}}_{a/N}(x,z,Q^2)$ describes the production of a hadron h in the hadronisation of a string that is formed by the struck quark and the target remnant. In contrast to the pQCD approach, this hadronisation function depends not only on quark and hadron types and on z but also on the type of the target nucleon and on x, see Ref. [14] for more details. We note that in this approach also the conservation of the overall quantum numbers as well as momentum conservation are taken into account, which is not the case for the pQCD approach. The LEPTO prediction for R_{K}, about 0.52, lies above the LO limit given by Eq. (5). However, for $z > 0.97$ it undershoots this limit. This appears plausible as for z approaching unity K^+ can be produced in the process $\mu\mathrm{p} \to \mu\mathrm{K}^+\Lambda^0$, while a similar process to produce K^- is forbidden because of baryon number conservation.

In recent years, several theory developments were performed that can potentially impact the theory predictions for the high-z region. In Ref. [15] for example, the authors studied the impact of threshold-logarithm resummations in the high-z region and found a large impact. In the case of π^- production, the predicted cross section can be larger by a factor of two. When considering the lower limit for R_{K}, the resummation corrections for K^- and K^+ are largely proportional to the PDF densities $\bar{\mathrm{u}} + \bar{\mathrm{d}}$ and u+d, respectively. Therefore, the R_{K} predictions including these resummation corrections would be even closer to the expectations given by Eq. (5) than the NLO predictions shown below without including these corrections. An interesting work related to hadron-mass corrections [16] was originally criticised in Ref. [17], but the discussion is ongoing [18]. The approach discussed in this work allows one to obtain a value of R_{K} below the limits discussed above. However, this approach seems to go beyond the standard factorisation theorem and corrections to $D^{\mathrm{h}}_{\mathrm{q}}$ are needed, which depend on the type of target nucleon and produced hadron h. There were also other developments, *e.g.* Refs. [19–21], which are very important for a better understanding of the hadronisation process. Still, they appear to not effectively impact the predictions for R_{K} in the high-z region at COMPASS kinematics.

3 Experimental set-up and data selection

The data were taken in 2006 using a μ^+ beam delivered by the M2 beam line of the CERN SPS. The beam momentum was 160 GeV/c with a spread of $\pm$ 5%. The solid-state ^{6}LiD target is considered to be purely isoscalar, neglecting the 0.2% excess of neutrons over protons due to the presence of additional material in the target (^{3}He and ^{7}Li). The target was longitudinally polarised but in the present analysis the data are averaged over the target polarisation, which leads to an effectively vanishing target polarisation on a level of better than 1%. The COMPASS two-stage spectrometer has a polar angle acceptance of $\pm$180 mrad, and it is capable of detecting charged particles with momenta above 0.5 GeV/c. The ring-imaging Cherenkov detector (RICH) was used to identify pions, kaons and protons. Its radiator volume was filled with C_4F_{10} leading to a threshold for pion, kaon and proton identification of about 3 GeV/c, 9 GeV/c and 18 GeV/c respectively. Efficient pion and kaon separation is possible with high purity for momenta between 12 GeV/c and 40 GeV/c. Two trigger types were used in the analysis. The "inclusive" trigger

[2] LEPTO 6.5, with JETSET 7.4 and fragmentation tuning from Ref. [13].

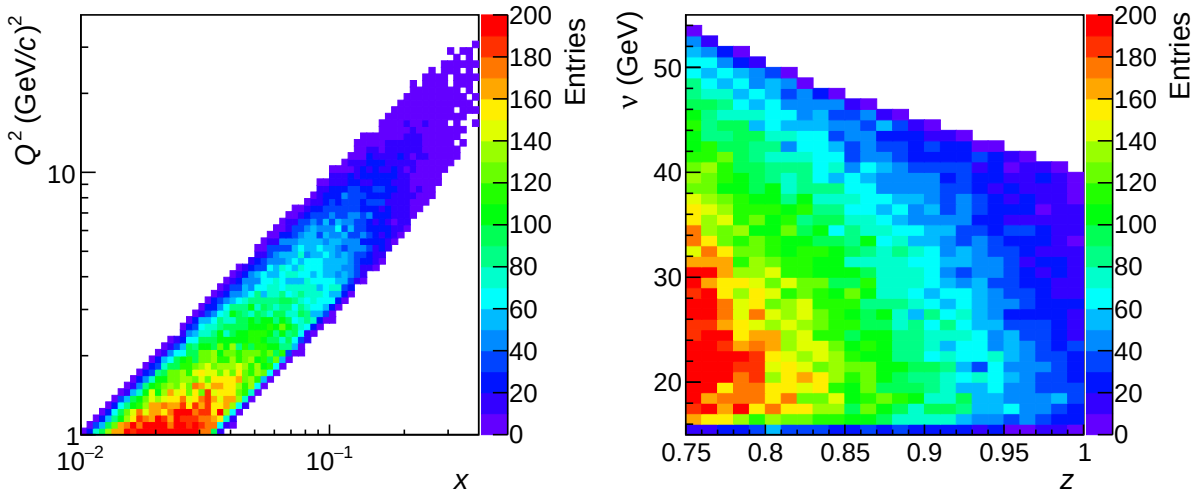

Fig. 1: Acceptance-uncorrected distributions of selected events in the (Q^2, x) plane and in the (ν, z) plane.

was based on a signal from a combination of hodoscope signals from the scattered muon. The "semi-inclusive" trigger required an energy deposition in one of the hadron calorimeters. The experimental set-up is described in more detail in Ref. [22].

The data selection criteria are kept similar to those used in the recently published analysis [3], whenever possible. The kinematic domain $Q^2 > 1$ (GeV/c)^2 and $W > 5$ GeV/c^2 is selected, thereby restricting the analysis to the region of deep inelastic scattering where pQCD can be applied. For small values of y, *i.e.* the fraction of the incoming muon energy carried by the virtual photon, the momentum resolution is degraded. In order to exclude this region, y is required to have a minimum value of 0.1. The aim of this analysis is to study kaon production in SIDIS for kaons carrying a large fraction z of the virtual-photon energy, hence it is restricted to $z > 0.75$. Using the above given momentum range for efficient kaon identification together with the large-z requirement in this analysis leads to an effective upper limit for y of 0.35.

The kaon multiplicities $M^{\mathrm{K}}(x, Q^2, z)$ are determined from the kaon yields N^{K} normalised by the number of DIS events, N^{DIS}, and divided by the acceptance correction $A^{\mathrm{K}}(x,Q^2,z)$:

$$\frac{\mathrm{d}M^{\mathrm{K}}(x,Q^2,z)}{\mathrm{d}z} = \frac{1}{N^{\mathrm{DIS}}(x,Q^2)} \frac{\mathrm{d}N^{\mathrm{K}}(x,Q^2,z)}{\mathrm{d}z} \frac{1}{A^{\mathrm{K}}(x,Q^2,z)} \,. \tag{7}$$

Note that in this work "semi-inclusive" triggers can be used because a bias free determination of N^{DIS} is not needed, as the latter cancels in R_{K}.

All data taken in 2006 are used in the analysis; altogether about 64000 charged kaons are available in the region $z > 0.75$. Examples of acceptance-uncorrected distributions of selected events are presented in Fig. 1 in the (x, Q^2) and (ν, z) planes. Here, ν is the energy of the virtual photon in the laboratory frame.

4 Analysis method

The analysis is performed in two x-bins, below and above $x = 0.05$, as already mentioned in Section 2. In each x-bin, five bins are used in the reconstructed z variable (z_{rec}) with the bin limits 0.75, 0.80, 0.85, 0.90, 0.95, 1.05. Since the RICH performance depend upon the momentum of the identified kaon, we also study R_{K} in bins of this variable using the bin limits 12 GeV/c, 16 GeV/c, 20 GeV/c, 25 GeV/c, 30 GeV/c, 35 GeV/c, 40 GeV/c. Note that in this way the ν dependence of R_{K} is studied implicitly and that the results are also given as a function of ν in these kaon-momentum bins.

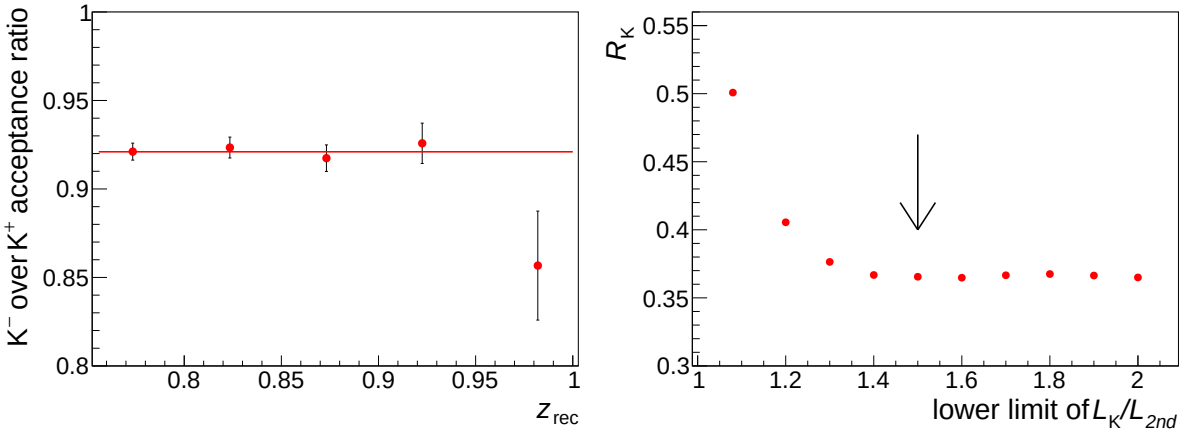

Fig. 2: Left: The K^- over K^+ acceptance ratio in the first x-bin, *i.e.* $x < 0.05$, as a function of the reconstructed z variable, as obtained from a Monte Carlo simulation. Right: The charged-kaon multiplicity ratio in the first x-bin, as a function of the lower limit of the RICH likelihood ratio for kaons with momenta between 35 GeV/c and 40 GeV/c. The arrow marks the value used in the analysis (see text for more details).

In order to determine the multiplicity ratio R_K from the raw yield of K^- and K^+ mesons, several correction factors have to be taken into account. First, the number of identified kaons is corrected for the RICH efficiencies. Based on studies of $\phi \to K^+K^-$ decays, where the ϕ meson was produced in a DIS process, the efficiency ratio for the two charges is found to be 1.002 ± 0.012. Such a simple "unfolding" procedure can be followed because a strict selection of kaons is made, so that the probabilities of misidentification of pion and proton as kaon can be assumed to be zero (possible remaining misidentification probabilities are discussed in Section 5).

The acceptance correction factors A^K for the two kaon charges are determined using Monte Carlo simulations. In the previous COMPASS analysis [3], a simple unfolding method was used to determine these factors. For a given kinematic bin in (x,y,z), the acceptance was calculated as the ratio of the number of reconstructed events to that of generated ones. For a given event, reconstructed variables were used to count reconstructed events and generated variables to count generated events. In order to account for the strong z-dependence of the multiplicity in the large-z region, in this analysis the acceptance is unfolded as in Ref. [3] for x and Q^2 but not for z. Various methods for z unfolding were investigated in detailed studies, see appendix A for an example. The results presented in this Letter are obtained using the simplest version of z unfolding, *i.e.* unfolding only the dependence of R_K on z_{corr}. Here, z_{corr} denotes the reconstructed value of z in the experiment, corrected by the average difference between the generated and reconstructed values of z, where the latter are determined by Monte Carlo simulations. In the left panel of Fig. 2, the K^- over K^+ acceptance ratio obtained from x and Q^2 unfolding is shown as a function of the reconstructed z-variable in the first x-bin. It appears to be independent of z within statistical uncertainties and has a value of 0.921 ± 0.004 in the first x-bin and 0.969 ± 0.010 in the second x-bin.

The contamination by decay products of diffractively produced vector mesons is estimated using HEPGEN [23] and found to be negligible, see Fig. 2 in [3]. Only ϕ decays are simulated there since heavier vector mesons have cross sections smaller by a factor of about 10 and decay mostly in multi-body channels, which results in even smaller probabilities to produce kaons at large z.

The measured cross sections have to be corrected for radiative effects in order to obtain σ^{DIS} and σ^h. Since, $y < 0.35$ holds as explained above, the size of radiative corrections is expected to be small. In any case, σ^{DIS} cancels in R_K and in the TERAD code [24] used in COMPASS analyses the relative radiative correction is the same for K^+ and K^-, so that it also cancels in the ratio.

5 Systematic studies

The charged-kaon multiplicity ratios measured in this analysis are found to agree with the results of the previous analysis [3] in the overlap region of the z-ranges used in these two analyses ($0.75 < z < 0.85$). Results derived from data that were obtained using different triggers are found to agree with one another within 2%.

The most important correction factor is the K^- over K^+ acceptance ratio, which for the first x-bin is 0.921 ± 0.004, as obtained using Monte Carlo data. The COMPASS spectrometer is designed to be almost charge symmetric. In the case of pions, the acceptance ratio obtained from Monte Carlo simulations is 0.991 ± 0.003, *i.e.* very close to unity. In contrast, the acceptance ratio of kaons obtained from Monte Carlo is found to be significantly below unity. This difference between K^- and K^+ yields is caused by the non-negligible thickness of the COMPASS target, which amounts to about 50% of a hadron interaction length, combined with a considerably larger absorption cross section for interactions of negative kaons compared to positive ones, see *e.g.* the results on the $K^{\pm}$-deuteron cross section in Ref. [25]. Depending on the longitudinal position of the primary interaction point Z_{vtx}, the produced kaons traverse a varying thickness of the material contained in the 120 cm long target. As a result, more negative than positive kaons are absorbed when the interaction took place at the beginning of the target as compared to an interaction at the end of the target. It is verified that once the acceptance correction was applied, the obtained R_{K} ratio is flat as a function of Z_{vtx}. For the K^- over K^+ acceptance ratio a 2% systematic uncertainty is used; this value is dominated by possible trigger-dependent variations of the multiplicities mentioned in the previous paragraph.

The stability of R_{K} is tested on data using several variables that are defined in the spectrometer coordinate system. The most sensitive one is the azimuthal angle ϕ of the produced kaon. The direction $\phi = 0$ lies in the bending plane of the dipole magnets and points towards the side, to which positive particles are bent. Correspondingly, the direction $\phi = \pi/2$ points towards the top of the spectrometer. In certain cases the charged-kaon multiplicity ratio is found to vary by up to 25%, with particularly small values close to a peak at $\phi = 0$. This observation is accounted for by a systematic uncertainty that is taken as the difference between the multiplicity ratio measured over the full ϕ-range and the one measured for $|\phi| > 0.5$. Typically, the relative uncertainty related to this ϕ-dependence ranges between 3% and 11%, which makes it the dominant systematic uncertainty. Note that the values of this systematic uncertainty for different bins in z are strongly correlated, with a correlation coefficient of about 0.8.

Further systematic uncertainties may arise from the RICH identification procedure. The K^- over K^+ efficiency ratio is expected to be close to unity since the RICH detector is situated behind a dipole magnet of relatively weak bending power. Additional studies were performed on data concerning misidentification probabilities of pions and protons being identified as kaons by varying the ratio of the kaon likelihood, which is the largest of all likelihoods in the selected sample, to the next-to-largest likelihood hypothesis, L_{K}/L_{2nd}. The behaviour of R_{K} as a function of the lower limit for L_{K}/L_{2nd} is shown in the right panel of Fig. 2 for kaon candidates with momenta between 35 GeV/c and 40 GeV/c. The constraint $L_{\text{K}}/L_{2nd} > 1.5$ is used in the present analysis. From these studies, the systematic uncertainty of the RICH unfolding procedure of about 3%. It corresponds to the difference in R_{K} calculated from the final sample and the one, in which a non-zero π contamination is detected.

As the COMPASS muon beam is (naturally) polarised with an average polarisation of -0.80 ± 0.04, a spin-dependent contribution to the total lepton-nucleon cross section cannot be neglected a priori. This contribution is proportional to $\sin\phi_{\text{h}}$ and expected to be smaller than the spin-independent one, which is proportional to $\cos\phi_{\text{h}}$ and $\cos 2\phi_{\text{h}}$ [26]. Here, ϕ_{h} denotes the azimuthal angle between the lepton-scattering plane and the hadron-production plane in the centre-of-mass frame of virtual photon and nucleon. Studies performed for previous COMPASS measurements [2,3] show that these effects can be neglected when using ϕ_{h}-integrated multiplicities, as it is done in this analysis.

Altogether, the total relative systematic uncertainty on R_K is found to range between 5% and 12% depending upon the z-bin. The systematic uncertainties in different z-bins are highly correlated, *i.e.* the correlation coefficient is estimated to vary between 0.7 and 0.8.

6 Results and discussion

In Table 1, the results on the charged-kaon multiplicity ratio R_K are presented in bins of the reconstructed z variable for the two x-bins. The measured z-dependence of R_K can be fitted in both x-bins by simple functional forms, *e.g.* $\propto (1-z)^\beta$, $\beta = 0.71 \pm 0.03$. Dividing in every z-bin the value of the ratio measured in the first x-bin by the one measured in the second x-bin, a "double ratio" $D_K = R_K(x < 0.05)/R_K(x > 0.05)$ is formed that appears to be constant over all the measured z-range with a value $D_K = 1.68 \pm 0.04_{\text{stat.}} \pm 0.06_{\text{syst.}}$. It is interesting to note that the measured value agrees within uncertainties with D_K calculated using the LO MSTW08L PDF set, *i.e.* 1.56 ± 0.07. In Fig. 3, R_K is shown as a function of z_{corr} for the two x-bins, as well as D_K in the inset of the figure. As both data and LO pQCD calculation exhibit the same z-dependence when comparing the charged-kaon multiplicity ratios in the two x-bins, in what follows we concentrate only on the first x-bin, *i.e.* $x < 0.05$. Still, the conclusions presented in the remaining part of the Letter are valid for both x-bins.

In Fig. 4, the present results on R_K in the first x-bin are compared with the expectations from LO and NLO pQCD calculations and with the predictions obtained using the LEPTO event generator, which were all discussed in Section 2. For completeness, we note that in the second x-bin the typical R_K predictions are about 1.5–1.6 times smaller than in the first x-bin. It is observed that with increasing z the values of R_K are increasingly undershooting the expectations from LO and NLO calculations. The discrepancy between the COMPASS results and the NLO predictions reaches a factor of about 2.5 at the largest value of z. As the difference between the lower limit in LO and the NLO DEHSS prediction obtained under the assumption $D_{\text{str}} = 0$ is never larger than 20%, it is very unlikely that any prediction obtained at NNLO would be able to account for such a large discrepancy.

As already mentioned in Sect. 2, the presented pQCD calculations rely on the factorisation ansatz $\mathrm{d}^3\sigma^{\text{h}}(x,Q^2,z)/\mathrm{d}x\mathrm{d}Q^2\mathrm{d}z \propto \sum_a e_a^2 f_a(x,Q^2) D_a^{\text{h}}(z,Q^2)$. If this ansatz would not be applicable at COMPASS energies for large values of z, it may be incapable to describe the behaviour of kaon multiplicities in this kinematic region. This pQCD ansatz does not include higher-twist terms, which are proportional to powers $1/Q^2$, so that the respective correction should be smaller by a factor of about three in the second x-bin compared to the first x-bin. However, the discrepancy between COMPASS results and both LO and NLO predictions is observed to be the same in the two x-bins within experimental uncertainties. The observed discrepancy cannot be explained by the threshold resummations from Ref. [15], as discussed in Section 2. The usage of DSS fragmentation functions [7] in the LO ansatz presented in Ref. [16] leads to a decrease of the R_K prediction by about 25% in the last z bin. It is thus not enough to account for the observed discrepancy. However, larger changes could be obtained if FFs decrease to zero faster than expected in the DSS parametrisation. It is worth noting that in the LEPTO event generator a different factorisation approach is used, which is based on string hadronisation. However, it does not describe the data at high z, in spite of its considerably higher flexibility in comparison to the pQCD approach. Perhaps a special tuning of certain string fragmentation parameters, for example those governing low-mass string hadronisation, would lead to a better description of the data.

In the analysis we assume that there is no contamination by decay products of vector mesons or by pions that were misidentified as kaons. Note that if these assumptions should not hold, the corrected R_K values would be further decreased with respect to the results presented in this Letter, *i.e.* the disagreement with pQCD expectations would be even stronger.

In Fig. 5, the dependence of R_K on the virtual-photon energy ν in bins of the reconstructed z variable is shown for the first x-bin. A clear ν-dependence of R_K is observed for all z-bins, except the last one.

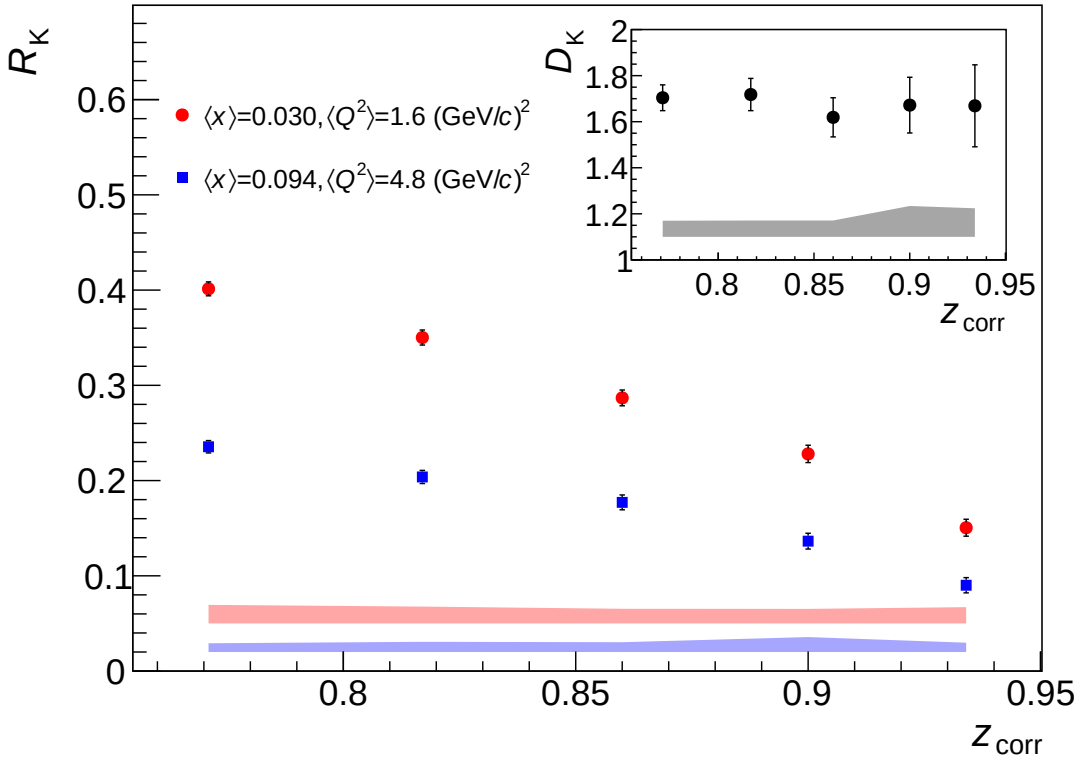

Fig. 3: Results on R_K as a function of z_{corr} for the two x-bins. The insert shows the double ratio D_K that is the ratio of R_K in the first x-bin over R_K in the second x-bin. Statistical uncertainties are shown by error bars, systematic uncertainties by the shaded bands at the bottom.

Table 1: Extracted values of R_K, bin limits of z (z_{min}, z_{max}), and the averages values of x, Q^2, z_{rec} and z_{corr} in first (upper part) and second (lower part) x-bin.

bin	x	Q^2 (GeV/c)^2	z_{min}	z_{max}	z_{rec}	z_{corr}	$R_K \pm \delta R_{K,stat.} \pm \delta R_{K,syst.}$
1	0.030	1.7	0.75	0.80	0.774	0.771	$0.401 \pm 0.007 \pm 0.019$
2	0.030	1.6	0.80	0.85	0.824	0.817	$0.350 \pm 0.008 \pm 0.018$
3	0.031	1.6	0.85	0.90	0.873	0.860	$0.287 \pm 0.008 \pm 0.015$
4	0.031	1.6	0.90	0.95	0.923	0.900	$0.228 \pm 0.009 \pm 0.015$
5	0.032	1.5	0.95	1.05	0.982	0.934	$0.150 \pm 0.009 \pm 0.017$
1′	0.094	5.1	0.75	0.80	0.774	0.771	$0.235 \pm 0.007 \pm 0.009$
2′	0.094	4.8	0.80	0.85	0.824	0.817	$0.204 \pm 0.007 \pm 0.011$
3′	0.093	4.6	0.85	0.90	0.873	0.860	$0.177 \pm 0.008 \pm 0.010$
4′	0.093	4.4	0.90	0.95	0.923	0.900	$0.136 \pm 0.008 \pm 0.016$
5′	0.093	4.2	0.95	1.05	0.982	0.934	$0.090 \pm 0.008 \pm 0.010$

Within experimental uncertainties, the observed dependence on ν is linear and in the last bin a constant. Note that at most 15% of the observed variation of R_K with ν can be explained by the fact that in a given z-bin events at different ν have somewhat different values of x and Q^2. The observed strong ν dependence suggests that for larger values of ν the ratio R_K is closer to the lower limit expected from pQCD than it is the case for smaller values of ν. Numerical values for the ν dependence of R_K in bins of z_{rec} are given for both x-bins in Ref. [27].

In this analysis, the largest discrepancy between pQCD expectations and experimental results is observed in the region of large z and small y, *i.e.* small ν. As exactly in this region the previously published

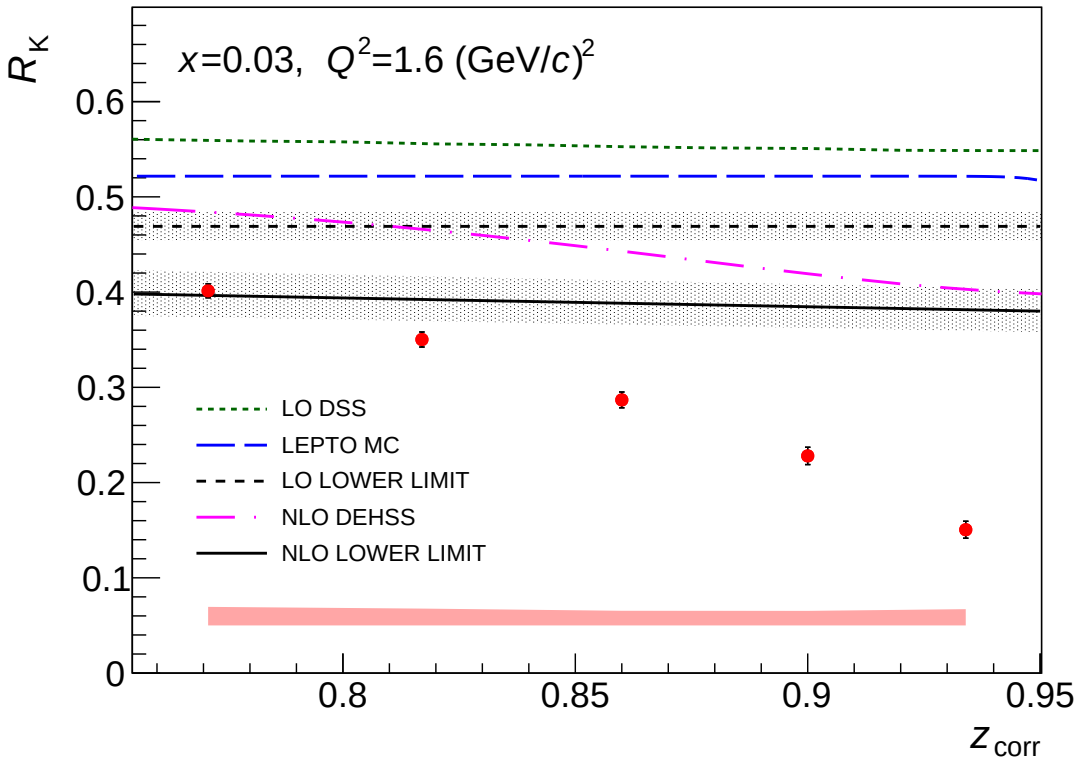

Fig. 4: Comparison of R_K in the first x-bin with predictions discussed in Section 2. The systematic uncertainties of the data points are indicated by the shaded band at the bottom of the figure. The shaded bands around the (N)LO lower limits indicate their uncertainties.

COMPASS data [3] had shown the largest tension with the NLO pQCD fits of FFs, see Section 1, the present results provide additional evidence that this tension is of physical origin.

The observed violation of the pQCD expectations for the charged-kaon multiplicity ratio at large values of z may be interpreted as follows. If the produced kaon carries a large fraction z of the virtual-photon energy, there is only a small amount of energy left to fulfil conservation laws as *e.g.* those for strangeness number and baryon number, which are not taken into account in the pQCD expressions for the SIDIS cross section. The larger the value of z, the smaller is the number of possible final states in the process under study. The natural variable to study the "exclusivity" of a process is the missing mass, which is approximately given by $M_X = \sqrt{M_p^2 + 2M_p\nu(1-z) - Q^2(1-z)^2}$. As the factor $\nu(1-z)$ appears in the missing mass definition, both the z and the ν dependence of R_K may be described simultaneously by this variable. Figure 6 shows that R_K as a function of M_X follows a rather smooth behaviour. The disagreement between our data and the pQCD predictions suggests that a correction within the pQCD formalism is needed in order to take into account the phase space available for the hadronisation of the target remnant. We observe that our data can be reconciled with the pQCD NLO prediction (R_K larger than about 0.4) only above the rather high M_X value of about 4 GeV/c^2, which is rather surprising (see *e.g.* Ref. [28]). Since the dominant term in M_X is $\propto \sqrt{\nu(1-z)}$, this observation also suggests that for experiments with accessible values of ν smaller than those at COMPASS, the disagreement with pQCD calculations and possible deviations from these expectations may already be observed at smaller values of z.

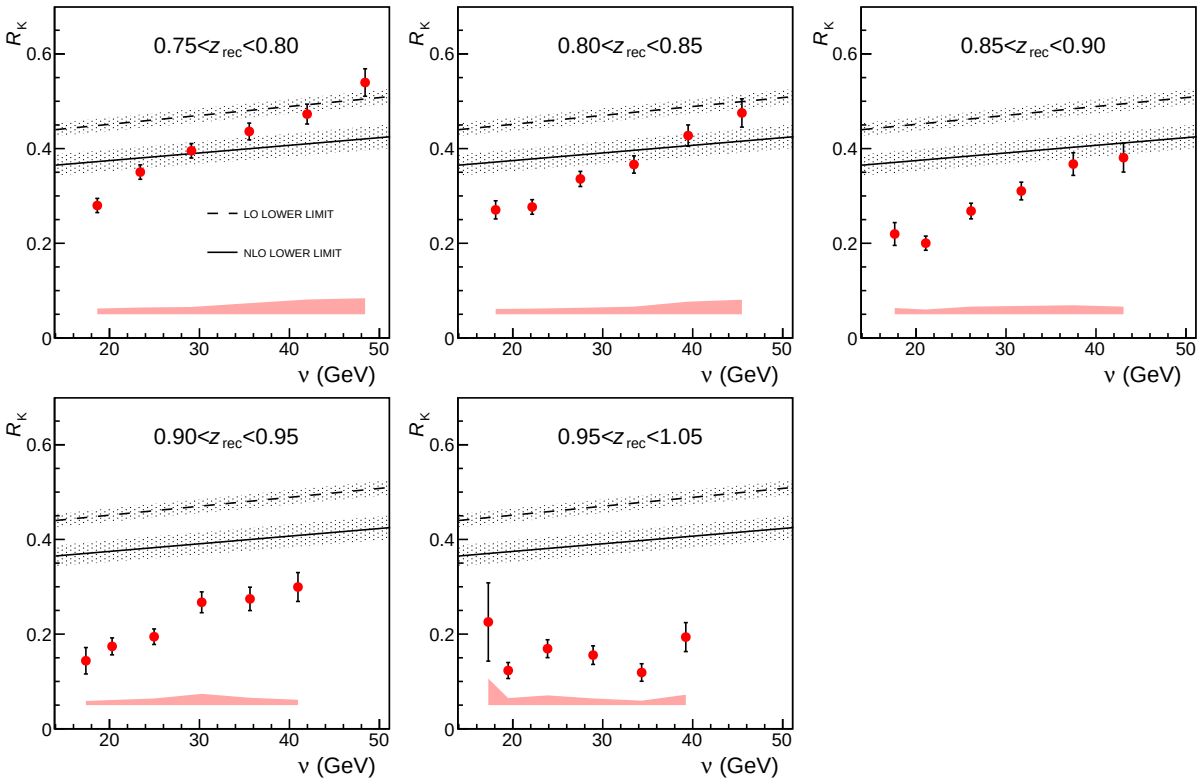

Fig. 5: The K^- over K^+ multiplicity ratio as a function of ν in bins of z, shown for the first bin in x. The systematic uncertainties of the data points are indicated by the shaded band at the bottom of each panel. The shaded bands around the (N)LO lower limits indicate their uncertainties.

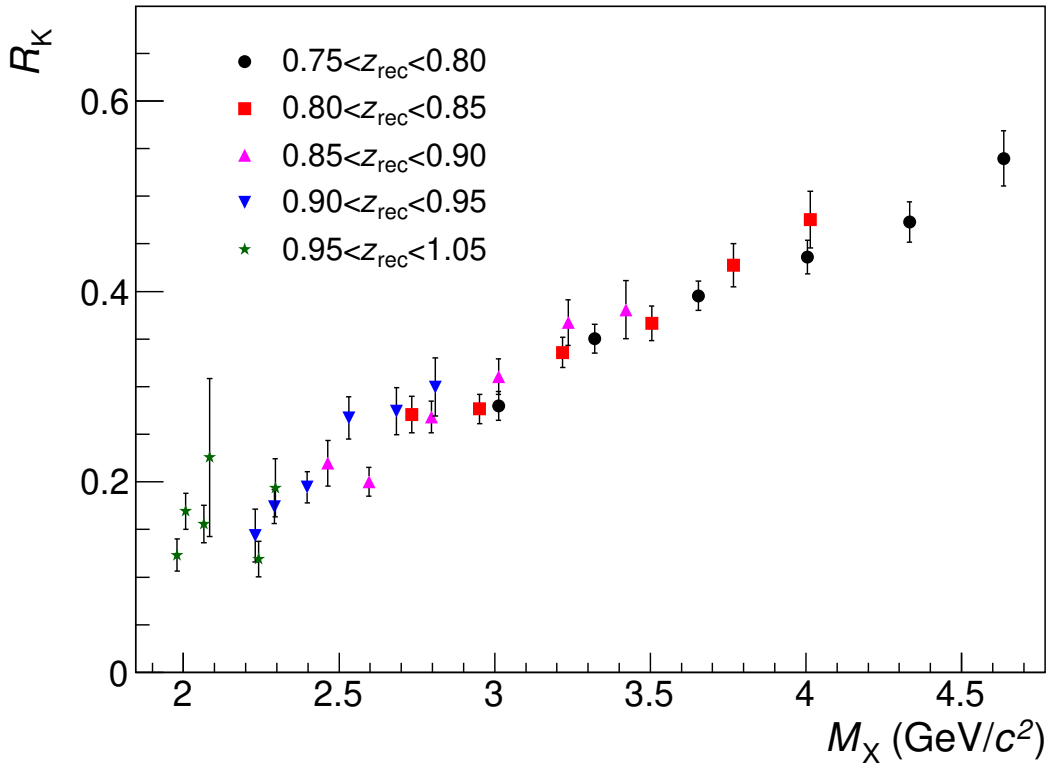

Fig. 6: The K^- over K^+ multiplicity ratio presented as a function of M_X. See text for details.

7 Summary

In this Letter, the K^- over K^+ multiplicity ratio R_K measured in deep-inelastic kaon leptoproduction at large values of z is presented for the first time. It is observed that the R_K values fall below the lower limits calculated at LO and NLO accuracy in the pQCD formalism. In addition, we observe that the kaon multiplicity ratio R_K strongly depends on the missing mass in the single-inclusive kaon production process. Altogether, our observations suggest that more theory effort may be required in order to understand kaon production at high z. In particular, within the pQCD formalism an additional correction may be required that takes into account the phase space available for hadronisation.

Acknowledgements

We would like to thank D. Stamenov for useful discussions. We gratefully acknowledge the support of the CERN management and staff and the skill and effort of the technicians of our collaborating institutes. This work was made possible by the financial support of our funding agencies.

A Procedure for z-unfolding

A typical unfolding procedure produces a covariance matrix with non-negligible off-diagonal matrix elements. These correlations are important and in many cases cannot be neglected, as it is also emphasised in Ref. [29]. In certain phenomenological analyses of published multiplicity data, however, these important pieces of information are erroneously neglected, which may lead to improper data treatment and thus to incorrect conclusions. In order to prevent such problems, we chose a simple unfolding method in our main analysis. We note that any correctly performed unfolding procedure can only decrease the value of R_K measured at a given value of z_{rec}, so that the choice of the unfolding procedure can not possibly explain the discrepancy observed between pQCD predictions and COMPASS results.

As an example of a more sophisticated z-unfolding method, a procedure is presented that assures a smooth behaviour of the resulting charged-kaon multiplicity ratio. Based on MC data a smearing matrix is created, in which the probabilities are stored that the kaon with a generated value z that belongs to a certain z_{gen}-bin is reconstructed in a certain z_{rec}-bin. The width of the z-bins is chosen to be 0.05 and values of z_{rec} up to 1.10 are studied. The obtained smearing matrix is given in Ref. [27] as supplemental material. In the next step, a functional form for the $K^\pm$ multiplicities is assumed in the 'true' phase space for data, which for MC data corresponds to the phase space of generated variables. For the fit of the real data, the functional form $\alpha \cdot \exp(\beta z)(1-z)^\gamma$ is used. This function is integrated in bins of z_{gen}, which are defined by the smearing matrix. In this way, a vector of expectation values is obtained in the 'true' phase space. This vector is multiplied by the smearing matrix, resulting in expectation values for kaon yields in the reconstructed phase space. The yield predictions obtained in this way are directly compared with the experimental values by calculating a χ^2 value. This value is minimised to find optimal parameters for the fitting function. In order to obtain the uncertainty of the unfolded ratio, the bootstrap method is used with 400 replicas of our data [30]. At a given value of z, the uncertainty of the ratio is taken as Root Mean Square from the replicas distribution. The effect of unfolding is rather small for all bins except the last one. The obtained results are summarised in Table A.1 and the correlation matrix is given in Table A.2.

References

[1] V.N. Gribov and L.N. Lipatov, Sov. J. Nucl. Phys. **15** (1972) 438; L.N. Lipatov, *ibid.* **20** (1975) 95; G. Altarelli and G. Parisi, Nucl. Phys. B **126** (1977) 298; Yu.L. Dokshitzer, Sov. Phys. JETP **46** (1977) 641.

[2] COMPASS Collaboration, C. Adolph *et al.*, Phys. Lett. B **764** (2017) 1.

Table A.1: The z-unfolded $R_{\rm K}$ defined as $\int_{z_{\rm min}}^{z_{\rm max}} \frac{{\rm d}M^{\rm K^-}}{{\rm d}z}{\rm d}z / \int_{z_{\rm min}}^{z_{\rm max}} \frac{{\rm d}M^{\rm K^+}}{{\rm d}z}{\rm d}z$, where $z_{\rm min(max)}$ denote bin limits in z. The data below (above) $x = 0.05$ are presented in the top (bottom) part of the table.

bin	$z_{\rm min}$	$z_{\rm max}$	$R_{\rm K} \pm \delta R_{\rm K,\,stat.} \pm \delta R_{\rm K,\,syst.}$
1	0.75	0.80	$0.416 \pm 0.009 \pm 0.018$
2	0.80	0.85	$0.360 \pm 0.010 \pm 0.017$
3	0.85	0.90	$0.289 \pm 0.009 \pm 0.014$
4	0.90	0.95	$0.200 \pm 0.014 \pm 0.011$
5	0.95	1.00	$0.085 \pm 0.022 \pm 0.007$
$1'$	0.75	0.80	$0.237 \pm 0.006 \pm 0.011$
$2'$	0.80	0.85	$0.202 \pm 0.006 \pm 0.010$
$3'$	0.85	0.90	$0.165 \pm 0.006 \pm 0.009$
$4'$	0.90	0.95	$0.123 \pm 0.009 \pm 0.007$
$5'$	0.95	1.00	$0.068 \pm 0.016 \pm 0.005$

Table A.2: The correlation matrix related to total uncertainties of the data presented in Table A.1.

bin	$1^{(\prime)}$	$2^{(\prime)}$	$3^{(\prime)}$	$4^{(\prime)}$	$5^{(\prime)}$
1	1.00	0.99	0.89	0.39	-0.18
2	0.99	1.00	0.94	0.47	-0.12
3	0.89	0.94	1.00	0.74	0.21
4	0.39	0.47	0.74	1.00	0.81
5	-0.18	-0.12	0.21	0.81	1.00
$1'$	1.00	0.98	0.84	0.37	-0.15
$2'$	0.98	1.00	0.93	0.50	-0.04
$3'$	0.84	0.93	1.00	0.78	0.30
$4'$	0.37	0.50	0.78	1.00	0.82
$5'$	-0.15	-0.04	0.30	0.82	1.00

[3] COMPASS Collaboration, C. Adolph *et al.*, Phys. Lett. B **767** (2017) 133.

[4] D. Stamenov, private communication (2017).

[5] W. Furmanski and R. Petronzio, Z. Phys.C **11**, (1982) 293.

[6] D. de Florian, M. Stratmann and W. Vogelsang, Phys. Rev. D **57** (1998) 5811.

[7] D. de Florian, R. Sassot and M. Stratmann, Phys. Rev. D **75** (2007) 114010.

[8] D. de Florian *et al.*, Phys. Rev. D **95** (2017) 094019.

[9] A. D. Martin, W. J. Stirling, R. S. Thorne and G. Watt, Eur. Phys. J. C **64** (2009) 653.

[10] L. A. Harland-Lang, A. D. Martin, P. Motylinski and R. S. Thorne, Eur. Phys. J. C **75** (2015) 204.

[11] NNPDF Collaboration, R. D. Ball *et al.*, J. High En. Phys. **04** (2015) 040.

[12] G. Ingelman, A. Edin and J. Rathsman, Comput. Phys. Commun. **101** (1997) 108.

[13] COMPASS Collaboration, C. Adolph *et al.*, Eur. Phys. J. C **77** (2017) 209.

[14] A. Kotzinian, Eur. Phys. J. C **44** (2005) 211.

[15] D. P. Anderle, F. Ringer and W. Vogelsang, Phys. Rev. D **87** (2013) 034014.

[16] J. V. Guerrero *et al.*, JHEP **1509** (2015) 169.

[17] E. Christova and E. Leader, Phys. Rev. D **94** (2016) 096001.

[18] J. V. Guerrero and A. Accardi, Phys. Rev. D **97** (2018) 114012.

[19] D. P. Anderle, M. Stratmann, and F. Ringer, Phys. Rev. D **92** 114017.

[20] D. P. Anderle, T. Kaufmann, M. Stratmann, and F. Ringer Phys. Rev. D **95** 054003.

[21] M. Epele, C. G. Canal, and R. Sassot, Phys. Rev. D **94** 034037.

[22] COMPASS Collaboration, P. Abbon *et al.*, Nucl. Instrum. and Meth. A **577** (2007) 455.

[23] A. Sandacz and P. Sznajder, arXiv:1207.0333.

[24] A. A. Akhundov, D.Yu. Bardin, L. Kalinovskaya and T. Riemann, Fortschr. Phys. **44** (1996) 373.

[25] Particle Data Group, C. Patrignani *et al.*, Chinese Physics C **40** (2016) 100001.

[26] COMPASS Collaboration, C. Adolph *et al.*, Nucl. Phys. B **886** (2014) 1046.

[27] The Durham HEPData Project, https://www.hepdata.net.

[28] M. Diehl, W. Kugler, A. Schafer and C. Weiss, Phys. Rev. D **72** (2005) 034034; Erratum: Phys. Rev. D **72** (2005) 059902.

[29] HERMES Collaboration, A. Airapetian *et al.*, Phys. Rev. D **87** (2013) 074029.

[30] B. Efron, "The Jackknife, the Bootstrap, and Other Resampling Plans", Philadelphia, Pa: Society for Industrial and Applied Mathematics, ISBN 9781611970319 (1982).